

Comparative Analysis and Fusion of MRI and PET Images based on Wavelets for Clinical Diagnosis

Jinu Sebastian, and G. R. Gnana King

Abstract—Nowadays, Medical imaging modalities like Magnetic Resonance Imaging (MRI), Positron Emission Tomography (PET), Single Photon Emission Tomography (SPECT), and Computed Tomography (CT) play a crucial role in clinical diagnosis and treatment planning. The images obtained from each of these modalities contain complementary information of the organ imaged. Image fusion algorithms are employed to bring all of this disparate information together into a single image, allowing doctors to diagnose disorders quickly. This paper proposes a novel technique for the fusion of MRI and PET images based on YUV color space and wavelet transform. Quality assessment based on entropy showed that the method can achieve promising results for medical image fusion. The paper has done a comparative analysis of the fusion of MRI and PET images using different wavelet families at various decomposition levels for the detection of brain tumors as well as Alzheimer's disease. The quality assessment and visual analysis showed that the Dmey wavelet at decomposition level 3 is optimum for the fusion of MRI and PET images. This paper also compared the results of several fusion rules such as average, maximum, and minimum, finding that the maximum fusion rule outperformed the other two.

Keywords—MRI; PET; multimodality medical image fusion; wavelet transform; brain tumor; Alzheimer's disease; YUV color space

I. INTRODUCTION

IMAGE fusion is the technique of integrating distinct or complementary information present in two or more input images into a single fused image that comprises relevant information than either of the input images. This technique is used widely in remote sensing, military applications, and, most importantly, medical image processing. Image fusion methods can be mainly of two types: multi-focus type as well as multimodality type. In multi-focus image fusion, two or more images obtained from a single imaging modality with focus at different points are combined to get a complete picture of the scene imaged. In multimodality image fusion, the complementary information in images obtained from multiple modalities is integrated to get a single fused image.

In recent years, medical imaging modalities like MRI, PET, SPECT, and CT are utilized extensively by radiologists and doctors for disease diagnosis and treatment. Each one of these imaging modalities provides images that contain a specific kind

of information. For example, CT is a structural imaging modality that gives a clear view of the body's skeletal structure. On the other hand, MRI is another structural imaging modality capable of showing soft tissues with very high contrast and hence widely used for tumor detection. MRI-CT fusion can be adapted to merge hard tissue and soft tissue information into a single image for easy diagnosis. Likewise, PET and SPECT are functional imaging modalities that show blood flow and metabolic activities occurring inside the body. However, they do not offer any information regarding the structure of the organ. Therefore, functional data is merged with structural data for a better diagnosis of the disease. Thus, the fusion of other multimodality images like PET-CT, PET-MRI, MRI-SPECT come into the picture.

Before performing image fusion, the input images have to be registered [1] such that they are spatially aligned well. The registration process includes steps like shifting, shearing, rotating of input images so that they are well aligned. Then, from each input image, the most relevant characteristics are extracted and transferred to the fused image. The fused images are composed of significant information than any of the input images that makes them helpful for special applications like clinical diagnosis, remote sensing.

II. RELATED WORKS

Medical image fusion is usually performed at three stages viz., pixel, feature, and decision levels. Information linked with the pixels is directly used in pixel-level fusion. Feature level fusion methods extract different attributes like shape, texture from the input images and form the output image. The high-level method is the decision level which uses categorization and recognition of objects.

Fusion methods are broadly categorized as spatial domain and transform domain. Commonly used spatial domain methods are average, maximum, minimum [2], Principal Component Analysis (PCA) [3], Intensity-Hue-Saturation (HIS) [4], Brovey transforms [5], etc. Important transform domain methods include discrete wavelet transforms (DWT) [6], discrete cosine transform (DCT) [7], stationary wavelet transforms (SWT) [8], Curvelet [9], Contourlet [10], non-subsampled contourlet transforms (NSCT) [11], and non-subsampled shearlet

Jinu Sebastian is with Sahrdaya College of Engineering and Technology, Thrissur, Kerala, India under APJ Abdul Kalam Technological University (e-mail: jinuannasebastian@gmail.com, jinu@sahrdaya.ac.in).

G. R. Gnana King is with Sahrdaya College of Engineering and Technology, Thrissur, Kerala, India under APJ Abdul Kalam Technological University (e-mail: gnanaking@sahrdaya.ac.in).



transforms (NSST) [12]. Averaging fusion rule tends to reduce the contrast of characteristics present in only one of the input images and can lead to blurring in the fused image. The maximum fusion rule can select pixels with the highest activity from the input images. It is useful in highlighting the brightest spots in the input image. The minimum fusion rule selects the least activity pixels. PCA extracts significant characteristics from images to avoid redundancy. They produce spectral degradation and are hence not preferred for medical image fusion. IHS method produces images of good visual quality but sometimes color distortions may occur. DWT produces fused images with high SNR and less spectral distortions making it suitable for medical image fusion. DWT has shift variance problems and their directionality is limited. DCT has the undesirable side effect of blurring and SWT is difficult to implement. Curvelets and contourlets are good for processing curved shapes and edges. Curvelets are complex and contourlets are shift variants. NSCT is shift-invariant and has high directionality but is very complex to implement. NSST has shift-invariance, multi-directionality, and less complexity than NSCT.

Deep Learning approaches, which first emerged in 2017, have been a prominent topic in this field of study. For fusing medical images, algorithms such as Convolutional Neural Network (CNN) [13]–[19], and U-Net Network are used. Other methods like Pulse Coupled Neural Network (PCNN) [20] Recurrent neural network (RNN) and Fuzzy logic[21] are receiving increasing interest by the researchers over the past few years.

Researchers used to be interested in spatial domain image fusion algorithms, but they resulted in a spatial and spectral distortion in the fused images. The researchers then shifted their attention to the transform domain methods, where the fusion of images takes place in the transform domain. Although transform domain approaches offer fewer distortions, they suffer from noise issues. As a result, researchers increasingly integrate spatial domain and transform domain methodologies to achieve superior outcomes. Some of the Hybrid image fusion techniques in the literature are explained in [22]. Many other methods are also available to obtain fused images of better quality.

The medical images can be fused in many ways. CT-MRI provide soft and hard tissue details together. PET-CT, PET-MRI and MRI-SPECT offers both anatomical and functional details into a single image [23].

III. METHODOLOGY

The images used for the study are downloaded directly from the Whole Brain Atlas database (<http://www.med.harvard.edu/aanlib/home.html>) which is a standard set of medical images for evaluating the performance of multimodality medical image fusion methods. The database was formed by Keith A. Johnson and J. Alex Becker at Harvard Medical School.

A. Motivation for MRI and PET image analysis

MRI, as discussed earlier, is a structural imaging modality that yields high-resolution images with excellent contrast between the soft tissues of the brain, and hence they are used widely for brain tumor detection. PET images are low-

resolution images compared to CT and MRI that will provide color information showing the metabolic activities occurring at the cellular level. Since a disease often begins at the cellular level, early detection of tumors and other abnormalities is possible with a PET scan. Malignant cells have a high metabolic rate relative to non-cancerous cells, therefore they appear as bright spots on PET scans that are easily detectable. CT and MRI scans can detect changes in a cell when the organ's anatomy is altered. Therefore, PET scans are crucial in the early detection of malignancies. So in this paper, PET images are fused with MRI images to obtain high-resolution images having good contrast among soft tissues. The complementary information contained in the input PET and MRI images is preserved in the fused image, allowing the clinician to make an early diagnosis of the disease and help in better treatment planning.

B. The Wavelet transform

The Wavelet transform is a multi-resolution tool that yields a time-frequency representation of the image. The mother wavelet, which is the wavelet function, and the father wavelet, which is the scaling function, are two functions used to represent wavelets. To create self-similar wavelet families, the mother wavelet goes through translation and scaling operations given by the equation,

$$\psi_{a,b}(t) = \frac{1}{\sqrt{a}} \psi\left(\frac{t-b}{a}\right), (a, b \in R), a > 0 \quad (1)$$

An image consists of rows and columns, and the wavelet transform is applied firstly on the image rows and later on the columns. The wavelet decomposition is performed with the help of high pass and low pass filters. The image gets divided into four spatial frequency bands which include three high-frequency bands high-low (HL), low-high (LH), and high-high (HH), and a low-frequency band low-low (LL). LL is the approximation component representing the fine details, whereas the others represent course details in the input image. Fig.1. shows the level 1 decomposition of a single image.

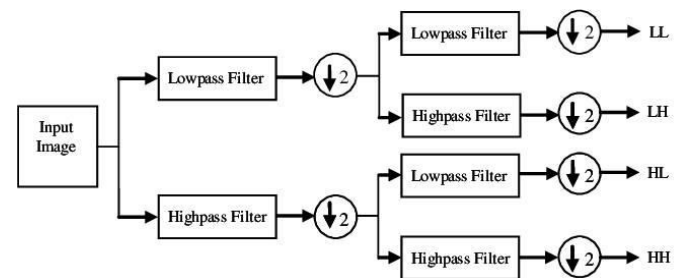


Fig.1. Level 1 decomposition of a single image

A) Wavelet families

Haar, Daubechies, Biorthogonal, Coiflets, Symlets, Morlet, Mexican Hat, and Meyer are the important wavelet families. We can find more details about them in [24].

C. Fusion Rules

The source images can be fused using linear fusion rules like averaging or non-linear fusion rules like maximum or minimum.

Let $M(x, y)$ be the input MRI image at coordinate (x, y) and $P(x, y)$ be the corresponding location in the PET image.

1) *Averaging Fusion Rule*

Here, the fused output image is created by taking the average of $M(x, y)$, and $P(x, y)$.

$$F(x, y) = [M(x, y) + P(x, y)]/2 \quad (2)$$

Averaging fusion rule tends to reduce the contrast of characteristics present in only one of the input images. Averaging can also lead to blurring in the fused image.

2) *Maximum Fusion Rule*

Here, the fused output image is created by choosing the pixel with the highest intensity value from the source images.

$$F(x, y) = \text{Max} \{M(x, y), P(x, y)\} \quad (3)$$

This method will select pixels with more activity from each of the input images.

3) *Minimum Fusion Rule*

Here, the fused output image is created by choosing the pixel with the lowest intensity value from the source images.

$$F(x, y) = \text{Min} \{M(x, y), P(x, y)\} \quad (4)$$

Apart from these three, other fusion rules also can be formulated based on the application.

D. *Quality Assessment*

Either qualitative or quantitative analysis can be used to assess the quality of the merged image. Qualitative analysis is done based on visual analysis of the fused image such as color, shape, etc. Quantitative analysis is of two types: with a reference image and without a reference image [25]. In the first type, the fused image quality is measured utilizing methods like Peak Signal to Noise Ratio and in the second type, the fused image quality is measured utilizing methods like entropy. In this paper, the quality assessment parameter used is entropy.

Entropy is the measure of information contained in an image. The expression for entropy is,

$$E = - \sum_{i=0}^{L-1} p_i \log_2 p_i \quad (5)$$

Where L is the image's number of intensity levels

$p = \{p_0, p_1, p_2, \dots, p_{L-1}\}$ is the distribution of probability levels

For an image with an 8-bit representation, the value of entropy varies between 0 and 8[17]. If the entropy value after the fusion process is higher, it implies that the algorithm has more information content and performs better.

E. *Image fusion algorithm based on Wavelet Transform*

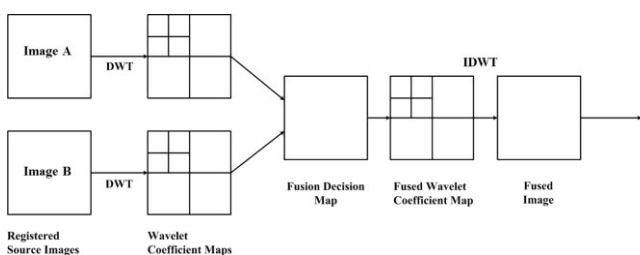


Fig. 2. Wavelet transform-based image fusion model

The wavelet transform-based image fusion model is in Fig. 2. Wavelet transform decomposes an input image into low frequency and high-frequency coefficients. As a result, the input image gets divided into LL, HL, LH, and HH sub-images. LL corresponds to low frequency or approximation coefficients, whereas the remaining sub-images correspond to high frequency or detail coefficients. In the second level of decomposition, low-frequency coefficients get further decomposed and the detail coefficients remain the same. Wavelet decomposition can be performed up to any level unless the image quality is degraded. After decomposition, appropriate fusion rules are used to combine the low frequency as well as high-frequency coefficients independently. The inverse wavelet transform is applied to get the final fused image. Fig.3. a) shows level 1 decomposition and Fig. 3. b) shows level 2 decomposition.

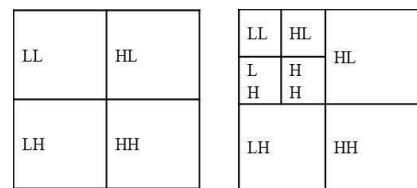


Fig. 3.a) level 1 decomposition b) level 2 decomposition

The low frequency and high-frequency coefficients are combined separately using different or the same fusion rules. The fusion rule can be linear or non-linear. An example for the linear fusion rule is averaging and that for the latter is maximum and minimum. Fusion rules can also be based on other criteria depending on the requirement. Once the fused image is formed in the transform domain, the final fused image in the spatial domain is generated using Inverse Wavelet Transform (IDWT).

F. *YUV color space*

Fusion of greyscale images with color images may result in color distortions. To avoid this, first, the color image is converted from RGB to YUV color space with Luminance (Y) and chrominance components U and V, where U is the blue projection and V is the red projection. The color information is present in chrominance components. The conversion formula is given below.

$$\begin{bmatrix} 0.299 & 0.587 & 0.114 \\ -0.147 & -0.289 & 0.436 \\ 0.615 & -0.515 & -0.1 \end{bmatrix} \begin{bmatrix} r \\ g \\ b \end{bmatrix} = \begin{bmatrix} Y \\ U \\ V \end{bmatrix} \quad (6)$$

Conversion from YUV to RGB is performed using the formula below.

$$\begin{bmatrix} 1 & 0 & 1.340 \\ 1 & -0.395 & -0.581 \\ 1 & 2.032 & 0 \end{bmatrix} \begin{bmatrix} Y \\ U \\ V \end{bmatrix} = \begin{bmatrix} r \\ g \\ b \end{bmatrix} \quad (7)$$

YUV is better for machine vision implementations than RGB due to the perceptual similarities to human vision[64].

G. *Proposed method*

We propose a novel method in which the input PET image is first converted from RGB space to YUV space forming the luminance (Y) and chrominance (U and V) components. Since the human eye is more sensitive to luminance, color information is filtered out from the PET image. The luminance component

of the PET image and the greyscale MRI image are then decomposed using DWT into low and high frequencies and individually combined using the maximum fusion rule. IDWT is applied to obtain the fused image in YUV space. Then the original U and V components are added to the fused image to get the final result in RGB space. Fig.4. shows the block diagram of the proposed method.

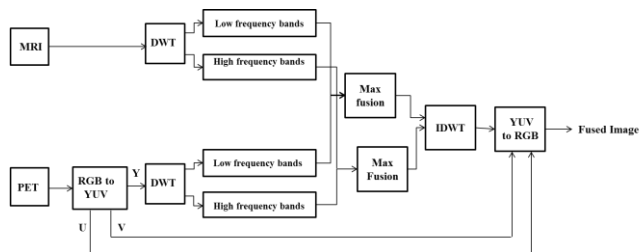


Fig. 4. Block diagram of the proposed method

II. RESULTS AND DISCUSSION

The source images obtained from the database are perfectly registered, which avoids the image registration step. MATLAB R2020a is used to implement the MRI-PET image fusion. The source images selected for the study are shown in Fig. 5.

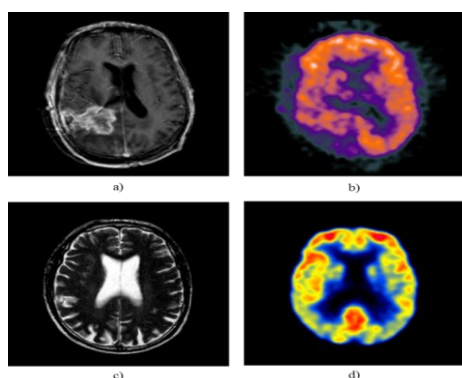


Fig. 5. a), b) source images for brain tumor detection c), d) source images for Alzheimer's disease detection.

Initially, the source PET and MRI images are fused using the fusion rules averaging, maximum, and minimum, and the results obtained are shown in Fig. 6. The quality of the fused image is measured using entropy. Parameter comparison and variation of parameters for different fusion rules are given respectively in Table I and Fig. 7.

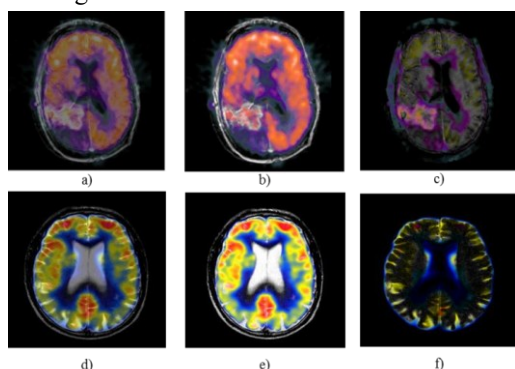


Fig.6. Results of applying different fusion rules. a) averaging b) maximum c) minimum fusion rules for brain tumor detection. d) averaging e) maximum f) minimum fusion rules for Alzheimer's disease detection.

TABLE I
PARAMETER COMPARISON USING DIFFERENT FUSION RULES

Fusion rule used	Entropy	
	Brain Tumor	Alzheimer's Disease
Average fusion rule	4.9148	4.0098
Maximum fusion rule	5.5325	4.0269
Minimum fusion rule	4.1322	2.4223

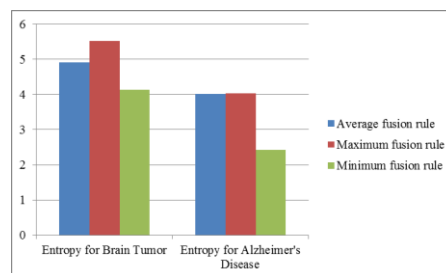


Fig. 7. Variation of entropy for different fusion rules

For comparing the performance of medical image fusion using different wavelet families, we have selected db2, sym4, coif2, Bior2.2, Rbio2.2, and Dmey. The decomposition levels compared are level 1 to level 5. The value of entropy for different wavelets at various decomposition levels for brain tumor detection is in TABLE II. The corresponding parameter variation is in Fig. 8. The comparison of entropy for different wavelets and the corresponding parameter variation are given respectively in TABLE III and Fig. 9 for Alzheimer's detection.

TABLE II
ENTROPY FOR DIFFERENT WAVELETS AT VARIOUS DECOMPOSITION LEVELS FOR BRAIN TUMOR DETECTION

Wavelet	L1	L2	L3	L4	L5
db2	5.5300	5.5281	5.5465	5.5706	5.7083
Sym4	5.5307	5.5269	5.5672	5.6370	5.9206
Coif2	5.5301	5.5301	5.5629	5.6725	5.8609
Bior2.2	5.5340	5.5354	5.5512	5.5975	5.7061
Rbio2.2	5.5246	5.5034	5.4873	5.5069	5.6872
Dmey	5.5384	5.5801	5.7739	6.0275	6.1226

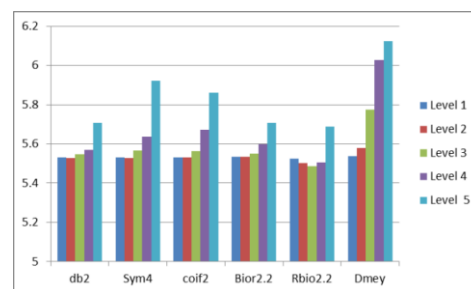


Fig.8 Variation of entropy for different wavelets at various decomposition levels for brain tumor detection

TABLE III
ENTROPY FOR DIFFERENT WAVELETS AT VARIOUS DECOMPOSITION LEVELS FOR ALZHEIMER'S DETECTION

Wavelet	L1	L2	L3	L4	L5
db2	4.1131	4.1632	4.2357	4.464	4.6714
Sym4	4.1213	4.2219	4.3349	4.6258	4.7922
Coif2	4.1288	4.2138	4.3159	4.6753	4.7427
Bior2.2	4.0808	4.1595	4.1595	4.4618	4.7524
Rbio2.2	4.1068	4.1340	4.1444	4.4136	4.5915
Dmey	4.2259	4.4113	4.8151	5.1401	5.2459

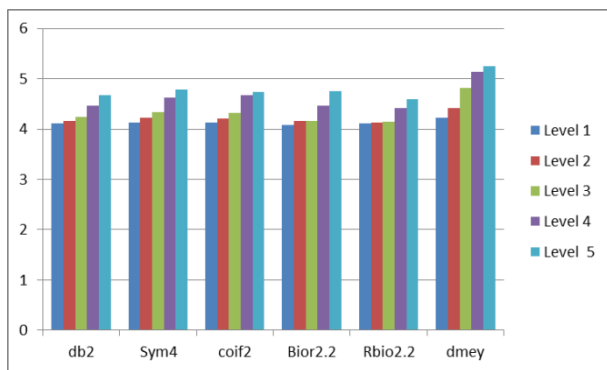


Fig.9 Variation of entropy for different wavelets at various decomposition levels for Alzheimer's detection

It is evident from TABLE I that the maximum fusion rule produces improved fused image quality compared to other fusion rules in terms of entropy. It means that the amount of information content is more when fused using the maximum rule. The visual analysis in Fig. 6 also proves that the maximum fusion rule produces high contrast fused images and is hence suitable for medical image fusion. Salient features like edges, region boundaries, and color information representing cell activity are better retained by using the maximum fusion rule. Therefore, in the comparative analysis, the maximum fusion rule is adopted for fusing the low frequency and high-frequency coefficients of the wavelet decomposition. The averaging fusion rule tends to diminish the contrast of the fused image while simultaneously blurring it. The minimum fusion rule offers less information than the other two in terms of objective and subjective analysis.

From Table II and Table III, the maximum entropy value is achieved for the Dmey wavelet at level 5 which means the maximum amount of information can be retained when fusion is done using the Dmey wavelet at decomposition level 5 compared to other wavelets. Dmey (Discrete Meyer) is symmetric, orthogonal, and biorthogonal, whereas Daubechies is an asymmetric wavelet. Coiflets and symlets are nearly symmetric, but Bior and Rbio are not orthogonal wavelets. The minimum entropy value is obtained for Bior2.2 at level 1. Therefore, the Dmey wavelet performs better than others for PET-MRI image fusion.

Dmey wavelet fusion is used to study the effect of decomposition levels on image fusion. Fig. 10 shows the results

of wavelet fusion using Dmey wavelet for brain tumor detection and Alzheimer's disease detection for levels 1 to 5.

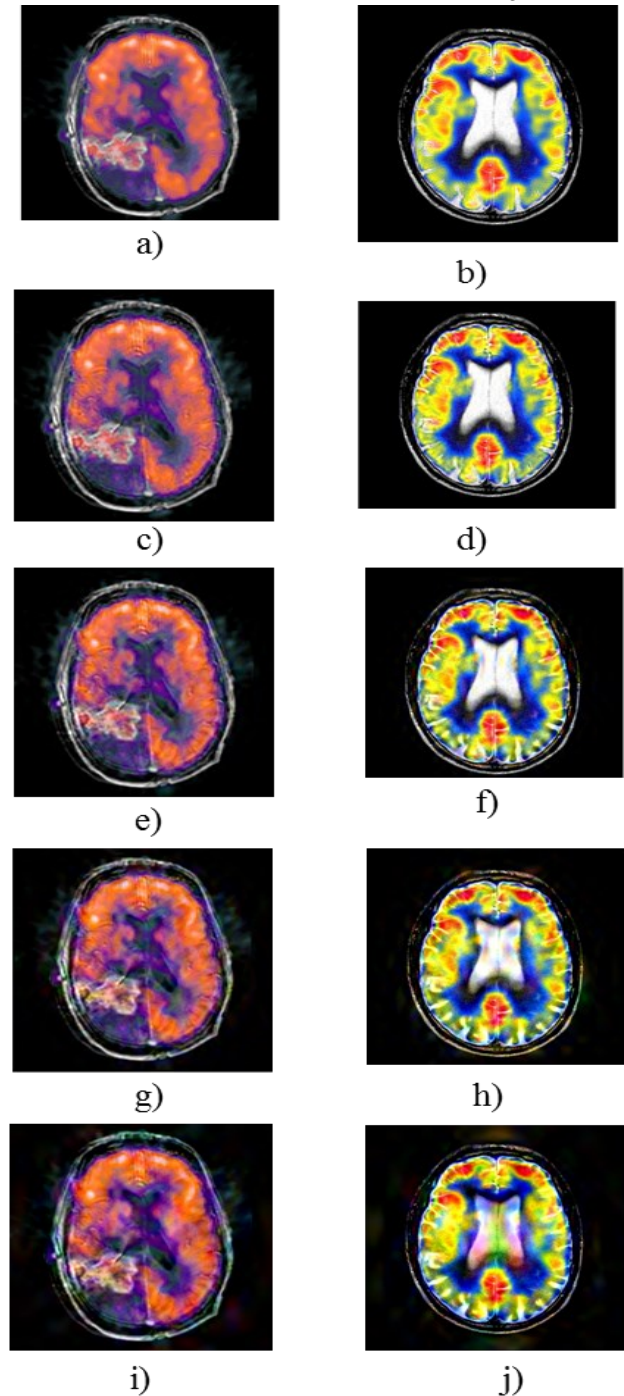


Fig.10. a), c), e), g), i) Results of wavelet fusion using Dmey wavelet for Brain tumor detection from levels 1 to 5. b), d), f), h), j) Results of wavelet fusion using Dmey wavelet for Alzheimer's disease detection for levels 1 to 5

Table II and Table III show that when the decomposition level increases, the entropy also increases, indicating an increase in the amount of information. The visual analysis in Fig. 10 shows that as the decomposition level increases, the edge features become more evident but, when the decomposition level goes beyond 3, some blocking artifacts get introduced in the fused image that tends to distort it. Moreover, with an increase in decomposition level, the complexity and the computation time of the fusion process are increased. So as a

tradeoff between all these parameters, this paper selected the optimum decomposition level for MRI and PET image fusion as level 3. At level 3 also the Dmey wavelet gives better results than the other wavelet families.

The proposed method uses the Dmey wavelet at level 3 for decomposition. The method is compared with other methods like PCA, IHS, DWT, PCA+IHS, PCA+DWT, and IHS+DWT. Fig. 11. shows the visual analysis for brain tumor detection and that for Alzheimer's disease detection is in Fig. 12. From the visual analysis, PCA, PAC+IHS, and PCA+DWT-based fusion produce low contrast images. The details are not visible. IHS method and IHS+DWT methods introduce color distortions in the fused image. DWT fusion and the proposed method produce comparable results in terms of visual analysis but the proposed method could attain fewer color distortions. The objective analysis in Table IV shows that the proposed method could achieve better results than the other methods.

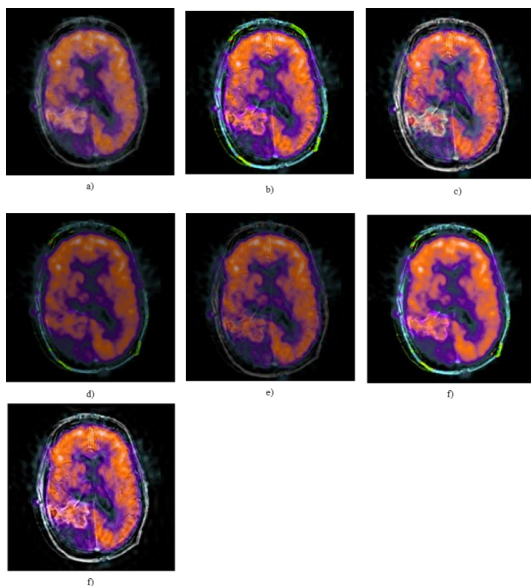


Fig. 11. Comparison for brain tumor detection a)PCA b)IHS c)DWT d)PCA+IHS e)PCA+DWT f)IHS+DWT g)Proposed

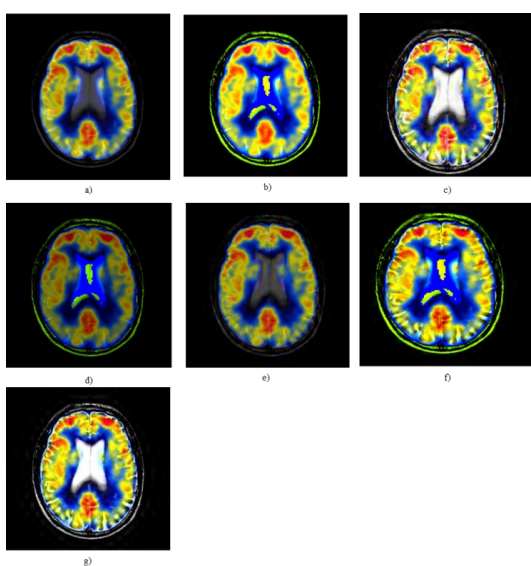


Fig. 12. Comparison for Alzheimer's disease a)PCA b)IHS c)DWT d)PCA+IHS e)PCA+DWT f)IHS+DWT g)Proposed

TABLE IV
COMPARISON OF PROPOSED METHOD WITH OTHER METHODS

Method	Entropy	
	Brain Tumor	Alzheimer's disease
PCA	5.0444	4.0638
IHS	5.4348	3.1387
DWT	5.7739	4.8151
PCA+IHS	4.9139	3.0900
PCA+DWT	5.3811	4.1962
IHS+DWT	5.7889	4.4671
Proposed	5.9118	4.9773

III. CONCLUSION

This paper proposes a novel fusion rule for MRI and PET images using YUV color space and the wavelet transform. The paper performs a comparative analysis of MRI and PET medical image fusion using different wavelet families at various decomposition levels. The effect of decomposition level on fused image quality is also analyzed. Quality assessment and visual analysis showed that the optimum decomposition level for MRI and PET image fusion is level 3. This paper also compared fusion rules such as averaging, maximum, and minimum, out of which the maximum fusion rule produced the best results in terms of entropy and visual perception. Therefore, for fusing the low and high-frequency coefficients of the wavelet transform, the maximum fusion rule is adapted. This method can be extended to other medical imaging modalities and also to multi-focus images. The drawback of the maximum fusion rule is that it is prone to noise and other artifacts as they possess a high value of intensities. The disadvantage of wavelet transform is that it lacks shift-invariance and directionality. So in our future work, we will resolve these issues by defining a new fusion rule and selecting NSST for decomposition, and improving the performance by training more data sets using deep learning.

REFERENCES

- [1] Chengazi, G. Flux, and G. Cook, "Image registration," *Clinical Nuclear Medicine* Fourth Edition. pp. 861–867, 2006, <https://doi.org/10.1201/b13348-88>
- [2] P. James and B. V. Dasarathy, "Medical image fusion: A survey of the state of the art," *Inf. Fusion*, vol. 19, no. 1, pp. 4–19, 2014, <https://doi.org/10.1016/j.inffus.2013.12.002>
- [3] D. K. Sahu and M. P. Parsai, "Different Image Fusion Techniques – A Critical Review," *Int. J. Mod. Eng. Res.*, vol. 2, no. 5, pp. 4298–4301, 2012.
- [4] M. Haddadpour, S. Daneshavar, and H. Seyedarabi, "PET and MRI image fusion based on a combination of 2-D Hilbert transform and IHS method," *Sci. Biomed. J.*, vol. 12, no. 6, pp. 1–7, 2017, <https://doi.org/10.1016/j.bj.2017.05.002>
- [5] O. S. Mishra and S. Bhatnagar, "MRI and CT Image Fusion Based on Wavelet Transform," *Int. J. Bio-Science Bio-Technology*, vol. 6, no. 3, pp. 149–162, 2014, <https://doi.org/10.14257/ijbsbt.2014.6.3.18>
- [6] K. Chaitanya, G. S. Reddy, V. Bhavana, and G. S. C. Varma, "PET and MRI medical image fusion using STDCT and STSVD," in 2017 International Conference on Computer Communication and Informatics, ICCCI 2017, 2017, pp. 5–8, <https://doi.org/10.1109/ICCCI.2017.8117685>
- [7] Ashwanth and K. Veera Swamy, "Medical Image Fusion using Transform Techniques," *ICDCS 2020 - 2020 5th International Conference on Devices, Circuits and Systems*, no. 2. pp. 303–306, 2020, <https://doi.org/10.1109/ICDCS48716.2020.243604>

- [8] P. Tank, D. D. Shah, T. V. Vyas, and S. B. Chotaliya, "Image Fusion Based On Wavelet And Curvelet Transform," *IOSR J. VLSI Signal Process.*, vol. 1, no. 5, pp. 32–36, 2013, <https://doi.org/10.9790/4200-0153236>
- [9] F. Shabanzade and H. Ghassemian, "Combination of wavelet and contourlet transform for PET and MRI image fusion," in *19th CSI International Symposium on Artificial Intelligence and Signal Processing, AISP 2017*, 2017, vol. 2018-Janua, pp. 178–183, <https://doi.org/10.1109/AISP.2017.8324077>
- [10] L. da Cunha, J. Zhou, and M. N. Do, "The nonsubsampling contourlet transform Theory, design, and applications," *IEEE Trans. Image Process.*, vol. 15, no. 10, pp. 3089–3101, 2006, <https://doi.org/10.1109/TIP.2006.877507>
- [11] Rajalingam, R. Priya, and R. Bhavani, "Hybrid Multimodal Medical Image Fusion Using a Combination of Hybrid Multimodal Medical Image Fusion Using Combination of Transform Techniques for Disease Analysis Transform Techniques for Disease Analysis," in *Procedia Computer Science*, 2019, vol. 152, pp. 150–157, <https://doi.org/10.1016/j.procs.2019.05.037>
- [12] Yang, Y. Wu, Y. Wang, and Y. Xiong, "A novel fusion technique for CT and MRI medical image based on NSST," in *Proceedings of the 28th Chinese Control and Decision Conference, CCDC 2016*, 2016, pp. 4367–4372, <https://doi.org/10.1109/CCDC.2016.7531752>
- [13] Wang, M. Zheng, H. Wei, G. Qi, and Y. Li, "Multi-modality medical image fusion using convolutional neural network and contrast pyramid," *Sensors (Switzerland)*, vol. 20, no. 8, pp. 1–17, 2020, <https://doi.org/10.3390/s20082169>
- [14] R. Balakrishnan, "Multimodal Medical Image Fusion based on Deep Learning Neural Network for Clinical Treatment Analysis," *Int. J. ChemTech Res.*, vol. 11, no. 6, pp. 160–176, 2018, <https://doi.org/10.20902/ijctr.2018.110621>
- [15] Z. Guo, X. Li, H. Huang, N. Quo, and Q. Li, "Medical image segmentation based on the multi-modal convolutional neural network: Study on image fusion schemes," in *Proceedings - International Symposium on Biomedical Imaging*, 2018, pp. 903–907, <https://doi.org/10.1109/ISBI.2018.8363717>
- [16] H. Hermessi, O. Mourali, and E. Zagrouba, "Convolutional neural network-based multimodal image fusion via similarity learning in the shearlet domain," *Neural Comput. Appl.*, vol. 30, no. 7, pp. 2029–2045, 2018, <https://doi.org/10.1007/s00521-018-3441-1>
- [17] Y. Liu, X. Chen, J. Cheng, and H. Peng, "A medical image fusion method based on convolutional neural networks," in *20th International Conference on Information Fusion, Fusion 2017 - Proceedings*, 2017, pp. 18–24, <https://doi.org/10.23919/ICIF.2017.8009769>
- [18] Z. Guo, X. Li, H. Huang, N. Guo, and Q. Li, "Deep Learning-Based Image Segmentation on Multimodal Medical Imaging," *IEEE Trans. Radiat. Plasma Med. Sci.*, vol. 3, no. 2, pp. 162–169, 2019, <https://doi.org/10.1109/trpms.2018.2890359>
- [19] N. Of and H. Of, "Multi-modal Medical Image Fusion using Convolutional Neural Networks Bachelor thesis," no. May 1996, 2018.
- [20] Huang et al., "A New Pulse Coupled Neural Network (PCNN) for Brain Medical Image Fusion Empowered by Shuffled Frog Leaping Algorithm," *Front. Neurosci.*, vol. 13, no. March, pp. 1–10, 2019, <https://doi.org/10.3389/fnins.2019.00210>
- [21] Kesavan et al., "Fuzzy Logic based Multi-modal Medical Image Fusion of MRI-PET Images," *Int. J. Sci. Technol. Eng.*, vol. 2, no. 10, pp. 268–271, 2016.
- [22] Sebastian and G. R. G. King, "Fusion of Multimodality Medical Images-A Review," *2021 Smart Technologies, Communication and Robotics (STCR)*, 2021, pp. 1–6, <https://doi.org/10.1109/STCR51658.2021.9588882>
- [23] J. Sebastian, G.R. Gnana King. (2022). Analysis of MRI and SPECT Image Fusion in the Wavelet Domain for Brain Tumor Detection. In: Rout, R.R., Ghosh, S.K., Jana, P.K., Tripathy, A.K., Sahoo, J.P., Li, K.C. (eds) *Advances in Distributed Computing and Machine Learning. Lecture Notes in Networks and Systems*, vol 427. Springer, Singapore. https://doi.org/10.1007/978-981-19-1018-0_53
- [24] M. Misiti and J. Poggi, *Wavelet Toolbox TM 4 User's Guide*. MATLAB, 2009.
- [25] P. Jagalingam and A. Vittal, "A Review of Quality Metrics for Fused Image," *Aquat. Procedia*, vol. 4, no. Icwrcoc, pp. 133–142, 2015, <https://doi.org/10.1016/j.aqpro.2015.02.019>